



Sonophotocatalytic degradation of fast green in aqueous phase using undoped and nitrogen doped ZnO

Srishti Kumawat, Yogeshwari Vyas, Priyanka Chundawat, Kiran Meghwal and Chetna Ameta*

Photochemistry Laboratory, Department of Chemistry, M. L. Sukhadia University, Udaipur-313 002, Rajasthan, India

E-mail: chetna.ameta@yahoo.com

Manuscript received online 26 May 2020, accepted 25 July 2020

Nowadays, nanoparticles have proved their great potent to eliminate the toxic material already produced in environment via simple microwave induced synthesis. In these a fast and efficient synthesis of N-ZnO and undoped nanoparticles was performed by microwave irradiation. The main objective of present study is to obtain optimize condition for photocatalytic and sonophotocatalytic degraded dye i.e. (fast green). The morphology besides structure of nanoparticles were determined by FTIR (Fourier-transform Infrared Spectroscopy), energy dispersive X-ray (EDX), X-ray diffraction (XRD), Field Emission Scanning Electron Microscopy (FESEM), Ultraviolet-Visible (UV-Vis) spectroscopy and Transmission Electron Microscopy (TEM). A comparative evaluation of photocatalysis, sonocatalysis and sonophotocatalysis processes was done for fast green dye using visible light and ultrasound irradiation, separately and simultaneously. The oxidative degradation of fast green dye was studied under different operating conditions including pH, primary concentration of dye and initial quantity of catalyst. The degradation proficiency by N-ZnO (doped) was obtained greater when contrasted with the undoped ZnO. The complete dye decay occurs in 100 min with sonophotocatalytic treatment. The water quality parameters before and after the sonophotocatalytic treatment were monitored by water analyser. Isopropanol was used as a radical scavenger to confirm $\cdot\text{OH}$ radicals since primary energetic species in the effective destruction of the fast green dye.

Keywords: N-doped ZnO, photocatalysis, sonocatalysis, sonophotocatalysis.

Introduction

Due to rapid industrialisation, the accumulation of harmful and poisonous materials such as organic dyes has led to a significant rise in water pollution levels.

These organic compounds oppose biodegradation and are responsible for the generation of toxic secondary products which affects aquatic wildlife and human health¹. There has been a rising demand to treat the water polluted by these organic compounds especially fast green dye. Fast green dye is extensively used as food colorant by the cosmetics and drug industries. Nonetheless, fast green dye is highly toxic colorant having mutagenic and carcinogenic properties. It has adverse effect on human skin, eyes, respiratory tracts as well as aquatic life. Consequently it is essential to eradicate fast green pollutant from industrial effluent to protect the ecosystem. The conventional methods of treating wastewater treatment possess its own limitation to treat hazardous compounds such a huge time and apparatus. In order to accomplish that, semiconductor catalysis is seen be-

ing pertinent process because of its low cost, extraordinary capability and low secondary pollution². Currently, ZnO (pure) and ZnO (hybrid) established semiconductors are believed to be potential candidates for a number of marketable and high-tech uses like beauty products, optoelectronics, and sound wave devices^{3,4}. They have good catalytic efficiency, chemical and thermal stability⁵⁻⁸. But the fast recombination rates reduce their efficiency as a photocatalyst⁹. So to decrease the electron-hole recombination rate, different techniques have been adopted. One of them is to introduce impurities like metal or non-metal elements such as Ga, Mg, Al, Cr, Mn, Fe, Ni, Cu, N, S, C etc. to ZnO in order to achieve its new and unusual physical properties as a nanocatalyst.

One of the widely known techniques is the Advanced Oxidation Processes (AOP) for water treatment process for environmental remediation¹⁰⁻¹³. The combination of AOP's like photocatalysis and sonocatalysis works synergistically leading to better results like enhanced generation of non-selective free radicals, cleansing the surface of catalyst, im-

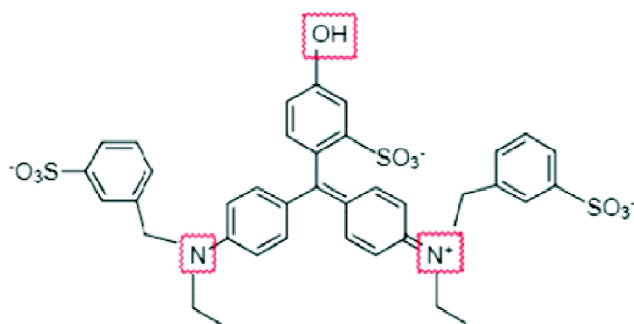
proved mass transfer, and removal of secondary pollution thus resulting in increased degradation rates of organic dyes^{14–19}.

Therefore in this work, a comparative study was done using different processes consisting of sonocatalysis, photocatalysis and sonophotocatalysis and the evaluation of degradation efficiency of fast green dye for each individual and combinational process using N doped ZnO (NZO) and undoped ZnO (ZO) was also investigated.

Experimental

Materials:

Zinc acetate dihydrate (ZAD) (SRL), hydrazine dihydrochloride (Thomas Baker), and NH₄OH solution, fast green FCF (FG) (Chemical structure of FCF is given in Structure No. 1) (HiMedia Laboratories Limited, Mumbai, India) were employed in the current study. Entire solutions were made in doubly distilled water (DDW).



Structure No. 1. Chemical structure of fast green dye.

Method:

Synthesis of N doped and undoped ZnO nanoparticles was executed by the wet chemical method using a microwave synthesizer²⁰ (Electrolux-EM 20 EC).

Instrumentation techniques:

The crystallinity of undoped and N-doped ZnO powder was confirmed by XRD using Rigaku Ultima IV with Cu K α irradiation in the range $2\theta = 10\text{--}90^\circ$. 40 kV is an accelerated voltage and the utilized current was 40 mA. FESEM studies exposed the Skelton of prepared NZO nanoparticles. For this Hitachi SU8010 FESEM was used. Transmission electron microscopy (TEM) examine on the microstructure of NZO was carried out on a TEM-Tecnai G2 20 instrument. UV-Visi-

ble reflectance mode spectra of prepared nanoparticles were inscribed in 200–800 nm wavelength range by Perkin-Elmer Lambda-750 UV-Visible spectrophotometer.

Sonophotocatalytic, sonocatalytic and photocatalytic-operation:

This analysis includes breakdown of fast green colorant, used as a contaminant was inspected in the existence of NZO nanoparticles using 200 W tungsten lamp (photocatalysis) and ultrasonic bath (sonocatalysis) arrangements separately and concurrently (sonophotocatalysis). A stock solution of FG ($10.0 \times 10^{-4} M$) was developed in DDW. Reaction suspension was prepared by adding 0.10 g of photocatalyst in 50 mL of $1.2 \times 10^{-5} M$ FG solution. This mixed solution was retained unlighted for an hour to construct an adsorption-desorption equilibrium on the photocatalyst before light irradiation. The solution was then irradiated with visible light using tungsten lamp (200 W). For the measurement of light intensity (in the unit of $mW\text{ cm}^{-2}$), a solarimeter (Model CEL 201) was used. The maximum light intensity was measured by varying the distance between the exposed surface of the reaction vessel and the filament of the lamp.

The sonophotocatalytic and sonocatalytic decay was expected by catalyst under ultrasonic bath (rectangular mould) filled with water run at a static frequency (40 kHz) and at 200 W power (ultrasonic). All runs were carried out under atmospheric conditions and by continuously stirring the reaction mixture. The pH of the solution was adjusted by the addition of previously standardized 0.1 N sulphuric acid and 0.1 N sodium hydroxide solutions. Prior to measurement of absorbance, NZO particles were separated using a centrifuge. Different water quality parameters like dissolve oxygen, salinity, TDS, conductivity and pH for adulterated and treated water were calibrated employing water analyser (Model 371, Systronics). The mineralization of FG was confirmed by evaluating the decline of COD (chemical oxygen demand) value. COD of FG dye solution was considered prior and later the sonophotocatalytic action with a typical dichromate process via COD digester. The percentage of sonophotodegradation proficiency (η) was evaluated using following equation:

$$\eta = \frac{\text{COD}_{\text{before}} - \text{COD}_{\text{after}}}{\text{COD}_{\text{before}}} \times 100 \quad (1)$$

Absorbance of samples was observed before starting the

run and at different intervals of time using UV-Visible spectrophotometer at 618 nm (λ_{\max} of fast green).

Results and discussion

We have characterized all the synthesized samples via various techniques which are briefly described below²⁰:

The XRD patterns (Fig. 1) suggested that average crystallite size for N-doped ZnO was 31.99 nm (Fig. 1b) whereas, for undoped ZnO, it was found to be 34.67 nm (Fig. 1a).

The FESEM micrographs of undoped (Fig. 2) and N-doped ZnO particles (Fig. 3) were uniform and have good regularity overall on observed surface. Upon closer examination, we observed that their structures were like nanorods.

Their FESEM micrographs (Fig. 2) reveal that the rods consisted of thinner plates stacked one above the other. With the introduction of N in the system (Fig. 3), these nanorods

became porous. They have “pencil like tip” at both ends. The nanorods were joined together to form nano-flower like structure.

EDS result of undoped ZnO nanoparticles (NPs) show 77.13 wt% of Zn and 22.87 wt% of O ions. Pure nature of ZnO NPs was confirmed by the witness of EDS signal since no extra signal obtained (Fig. 4a). Fig. 4a displays the Zn and oxygen composition only.

EDS spectroscopy for NZO (Fig. 4b) was also performed to confirm presence of N and compositional analysis of nanoparticles. The obtained results for N-ZnO revealed 0.75 wt% for N, 18.48 wt% for O, 80.77 wt% for zinc. This result confirms that incorporation of N atoms in zinc oxide lattice. TEM image and SAED pattern reveal that it has sharp spots suggestive of symmetrical orientation and polycrystalline

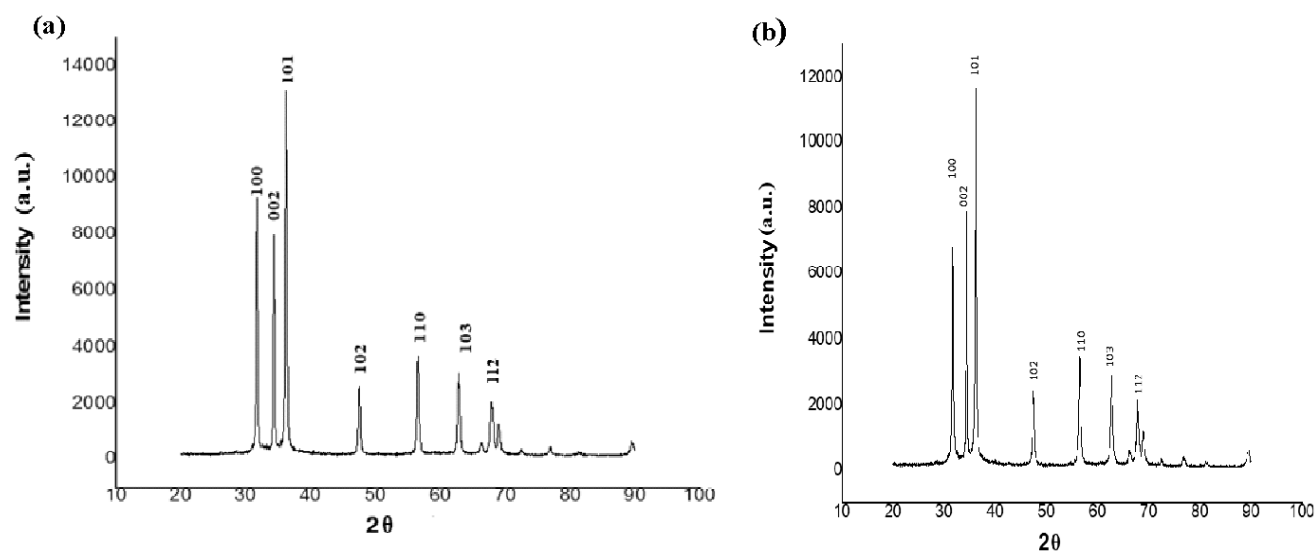


Fig. 1. (a) XRD of undoped ZnO, (b) XRD of N-doped ZnO.

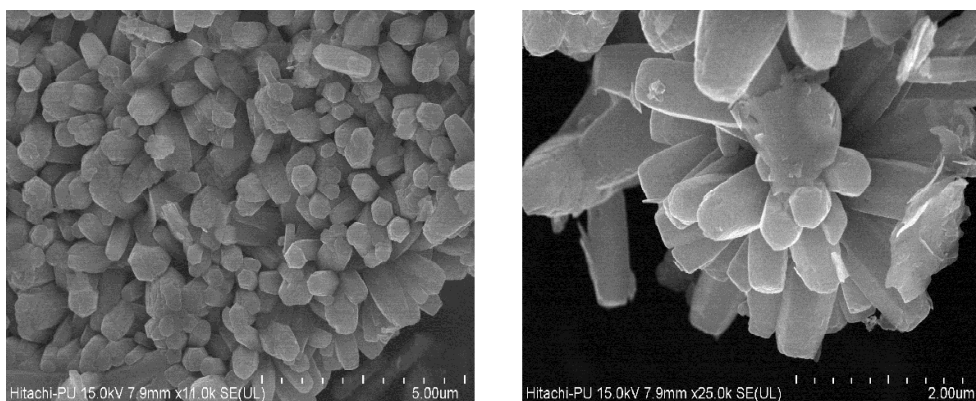


Fig. 2. FESEM images of undoped ZnO.

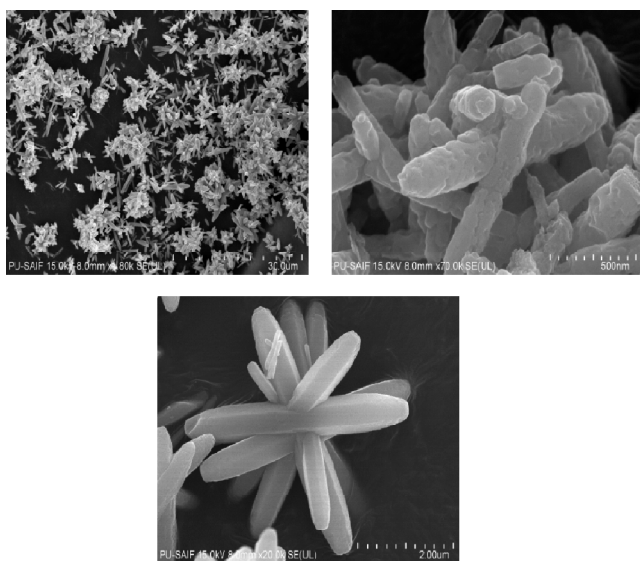


Fig. 3. FESEM images of N-doped ZnO.

behaviour of ZnO NPs in the sample. The diffuse reflectance UV-Vis spectra of undoped and N-doped ZnO showed that both catalysts can absorb visible light making it suitable to be used as photoactive catalyst under visible light irradiation. The optical band gap values for both samples were determined from reflectance spectra using the Kubelka-Munk equation

$$(K/S \times h\nu)^2 = A(h\nu - E_g) \quad (2)$$

where K/S is the so-called Kubelka-Munk function A is a constant depending on the transition probability, $(h\nu)$ is the incident photon energy. The values of $(K/S \times h\nu)^2$ vs (eV) were plotted as demonstrated in Figs. 5 and 6. Band gap energies

of undoped (Fig. 5) and N-ZnO (Fig. 6) were found to be 3.30 and 3.13 eV, respectively.

Therefore, N-doped ZnO absorbs longer wavelength visible light as compared to undoped ZnO, as band gap of NZO is low. N-doped ZnO expands the absorption range and reached to visible range.

A comparison for sonocatalysis (US), photocatalysis (VL) and sonophotocatalysis (US+VL) has been done and the results for degradation of fast green using ZO and NZO catalysts are presented in graphically presented in Fig. 7a (typical run).

The consequence of pH on the rate of disintegration of FG has been inspected in pH starting from 4.5 to 8.0 for undoped and N-doped ZnO catalysts while other parameters were kept alike. It was revealed that as pH increases, reaction speed enhances and after getting the extreme value i.e. pH 6.0 for all three systems, that is, sonocatalysis, photocatalysis and sonophotocatalysis, rate decreases with extra rise in pH. The outcomes are represented in graphs (Fig. 7b). The optimum rate of degradation at pH 6.0 (slightly acidic) reflected that degradation of protonated form of dye takes place. However, when pH is decreased from pH 6.0 to pH 4.5, concentration of protons in the medium increased, which gets adsorbed on the photocatalyst surface creating the surface of catalyst positively charged. Due to this, a force of repulsion is created between the catalyst superficial and protonated form of colorant, thereby retarding the rate of reaction with decrease in pH. On the other hand, rate also decreases when pH is increased from 6 to 8. It can be clarified by the fact that the comparative number of ions (OH^-) increases

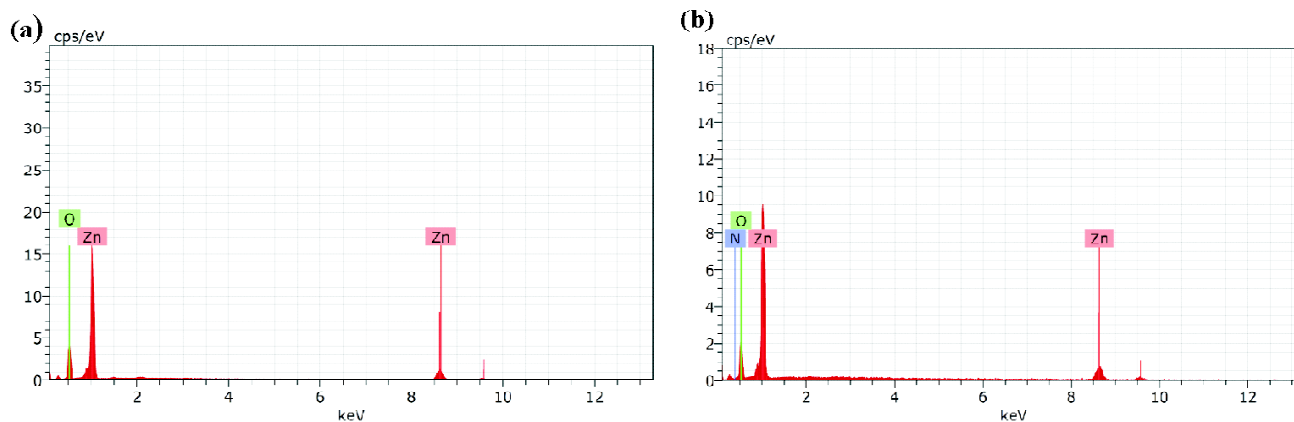


Fig. 4. (a) EDS image of undoped ZnO, (b) EDS image of N-doped ZnO.

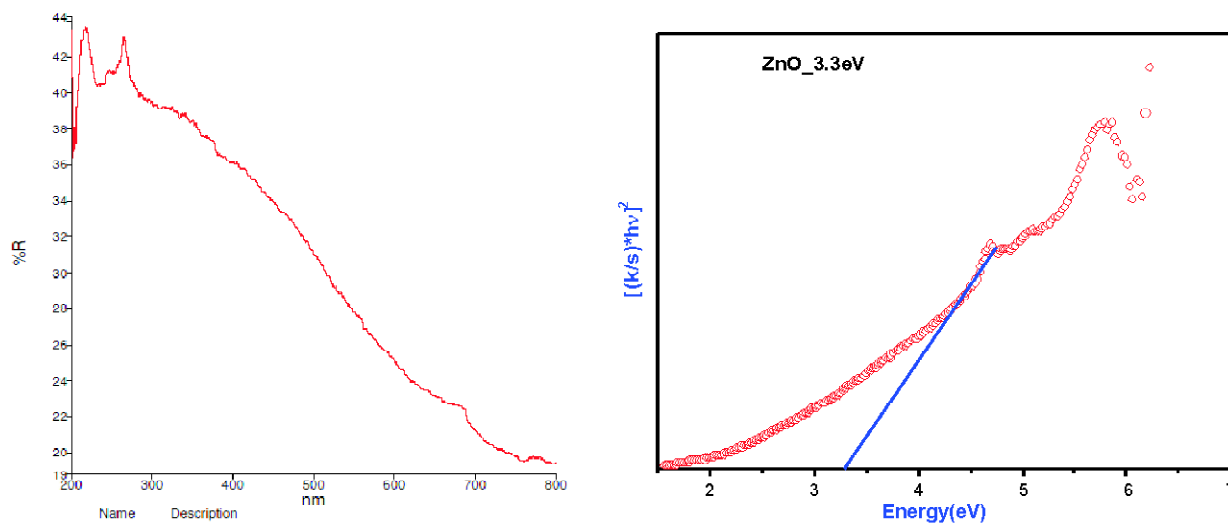


Fig. 5. UV-Vis reflectance spectrum of undoped ZnO.

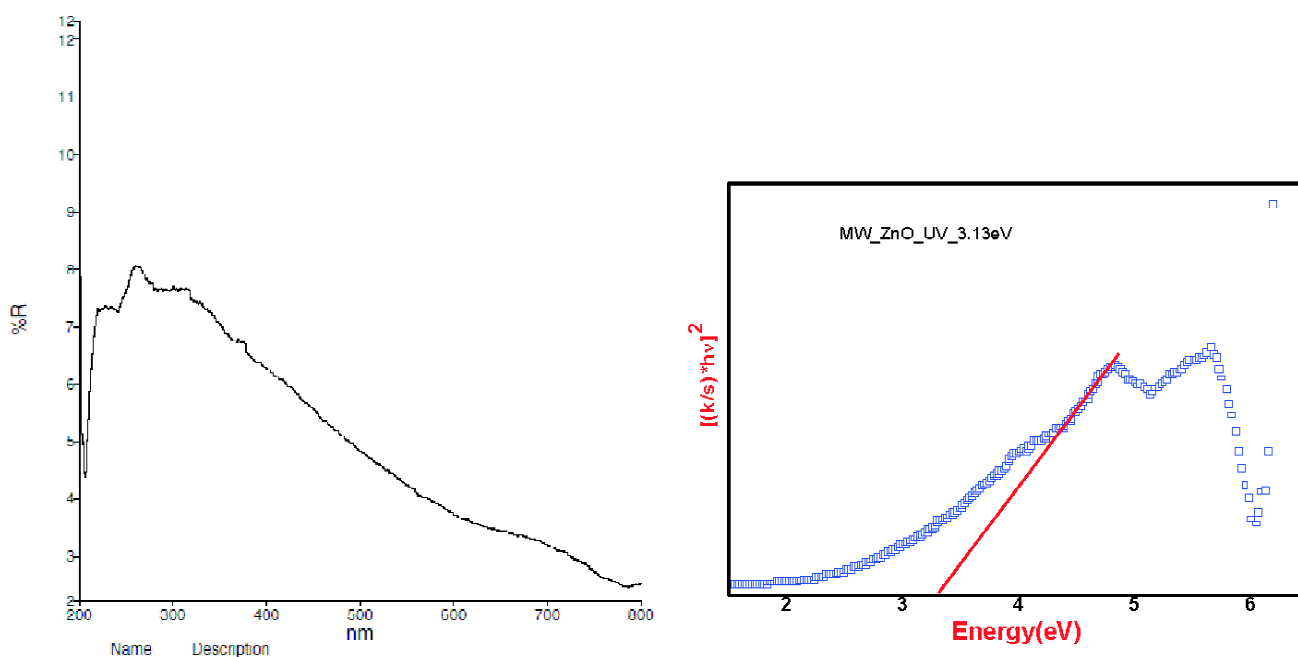


Fig. 6. UV-Vis reflectance spectrum of N-doped ZnO.

on changing the pH from 6.0 to 8.0, which make the surface negatively charged on increasing the concentration of OH^- ions. As a result, fewer amounts of anionic dye molecules will go towards the catalytic surface, thus, declining the reaction rate.

The maximum rate of degradation has been observed for sonophotocatalysis due to the cumulative synergistic ex-

posure of reaction mixture by light and US. For both catalysts, the rate constant follows the following order:

Sonophotocatalysis > Photocatalysis > Sonocatalysis

It has been observed that N-doped ZnO exhibited notably better activity for the degradation of FG dye as compared to undoped ZnO which might be probably subsequently narrowing of band gap energy from 3.37 eV to 3.13 eV.

Consequences of change in dye (FG) concentration on the speed of decay has been investigated by varying the dye concentration from $2 \times 10^{-6} M$ to $16 \times 10^{-6} M$ for undoped and N-doped ZnO catalysts keeping all other parameters identical. It has been observed that the rate of degradation increases with increase in concentration of dye up to $12 \times 10^{-6} M$ for sonocatalytic, photocatalytic and sonophotocatalytic processes for both catalysts. Rate decreases with additional increase in concentration after $12 \times 10^{-6} M$. The results are shown in Fig. 7c. Even for the variation of concentration of FG, the order of disintegration has been found to be sonophotocatalysis > photocatalysis > sonocatalysis. The highest rate of sonophotocatalysis clearly shows the synergistic effects of sonocatalytic and photocatalytic processes.

The variation effect on quantity of catalyst on the rate of FG degradation has been observed by varying the catalyst dosage from 0.04 g to 0.18 g during the sonocatalytic, photocatalytic and sonophotocatalytic treatment processes keeping all other parameters identical. It was detected that for both the undoped and N-doped ZnO catalysts, the degradation rate rises with rise in amount of the catalyst till a certain limit, which is 0.10 g and then starts to decrease on increasing the amount of catalyst beyond 0.10 g. Initially when the amount of catalyst is increased, the speed of degradation of colorant is also increased since increase in the number of active sites for the adsorption of colorant. The optimum amount of catalyst for highest k value was found at catalyst amount 0.10 g. However, beyond 0.10 g, extra increase in the catalyst amount, the retardation in degradation rate may be due to the catalyst's particles get clustered at its larger amounts thus triggering a fall in the number of active sites on the free surface of catalyst and thus decreasing the rate of dye degradation.

The light intensity variation on rate of decaying of dye was explored for sonophotocatalytic and photocatalytic processes by setting various other structures constant. The result showed that on enhancing the intensity of light, the reaction rate enhances and it was found highest at 60.0 mW cm^{-2} for both N-doped and undoped ZnO (Fig. 7e). As the intensity of light rises, the number of striking photons per unit area also rises, resulting in a higher decay rate. Advanced intensities of light are avoided because further raise in light intensity may trigger some thermal side reactions.

Various quality parameters were measured for sample

solution of FG dye before and after sonophotocatalytic treatment. Quality parameters were determined only for sonophotocatalysis because the best results for the disintegration speed of dye were obtained in sonophotocatalysis. The values of dissolved oxygen (DO), conductance, salinity,

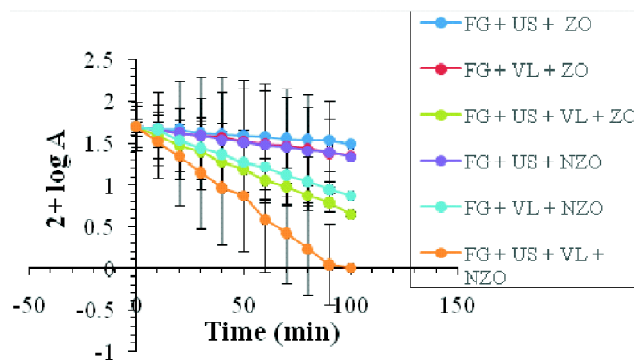


Fig. 7(a). Typical run.

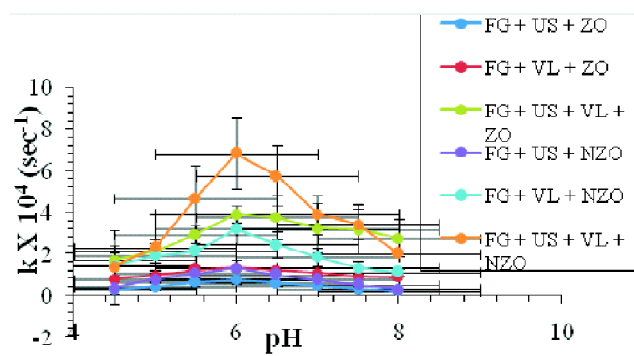


Fig. 7(b). pH consequence.

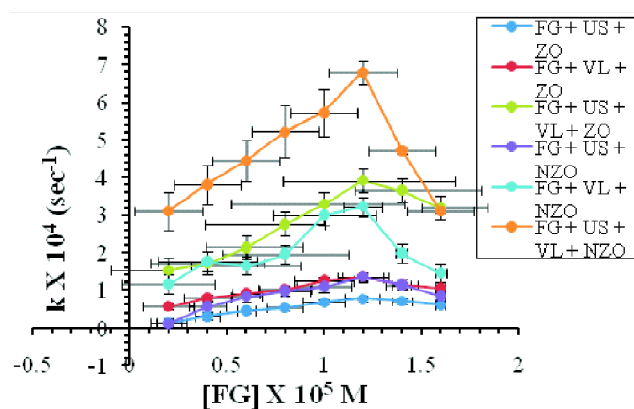


Fig. 7(c). Outcome of dye concentration.

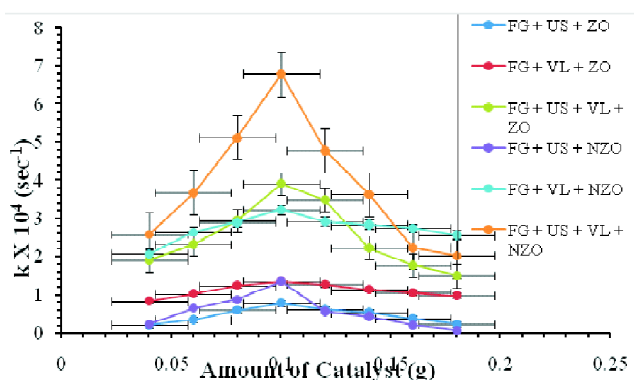


Fig. 7(d). Result of extent of catalyst.

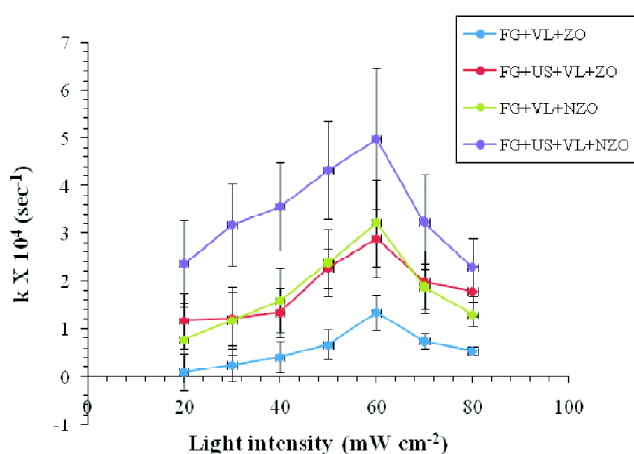


Fig. 7(e). Outcome of light intensity.

total dissolved solids (TDS), pH and chemical oxygen demand (COD) are given in Table 1.

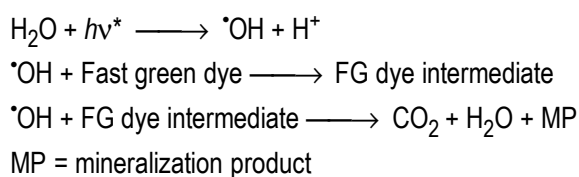
The COD value for dye solutions decreased from 525 mg L⁻¹ to 243.9 mg L⁻¹ (52.4% dye degradation) and 123.4 mg L⁻¹ (76.4%) for both undoped and doped catalysts, respectively after 100 min of irradiation.

Quantity of dissolved O₂ gas in water is measured with DO analysis. The amount of dissolved oxygen was 0.1 ppm for both undoped and N-doped ZnO before degradation. After sonophotocatalytic treatment, the amount of dissolved oxygen increased to 3.0 ppm and 4.2 ppm respectively, which specifies pollutant mineralization to a larger amount.

More the number of ions, the greater will be the conductivity and so, conductivity can be used as an estimate of the amount of ion concentration of a solution. Later the sonophotocatalytic action, conductivity increased which indicates that the dye was mineralized into smaller ions/molecules like SO₄²⁻, CO₂, NO₃⁻, etc. Due to the similar purpose, the TDS along with salinity of the dye solution increased.

Reaction mixture's pH was acidic earlier treatment however after sonophotocatalytic decay of the dye, pH turns nearly neutral. It clearly shows that the dye particles are mineralized to a greater extent.

Tentative mechanism of dye degradation is given in structure No. 2 where MP includes SO₄²⁻, NO₃⁻ radicals.



Structure No. 2. Mechanism of dye degradation.

Table 1. Water grade parameters

Numerous constraints	Prior treatment	Sonophotocatalytic	After treatment	Sonophotocatalytic
	ZO	NZO	ZO	NZO
COD (mg/L)	525	525	243.9	123.4
DO (ppm)	0.1	0.1	3.0	4.2
Conductance (μS)	30.5	30.5	231	432
Salinity (ppt)	0.02	0.02	0.12	0.28
TDS (ppm)	19.3	19.3	175	273
pH	5.4	5.4	6.57	7.34

Conclusions

N-doped ZnO is found to be more effective than undoped ZnO to mineralize the aqueous solution of fast green dye in the presence of light and ultrasound. The optimum degradation was found at pH 6, 1.2×10^{-5} M concentration of dye and 2.4 g L^{-1} of the catalyst. The degradation of fast green dye under sonophotocatalysis was more efficient than that under photocatalysis and sonocatalysis alone and all of these processes followed pseudo-first order kinetics. Fast green dye was selected since it used in various purposes and an unmanageable pollutant in the environment. It is utilized in quantitative stain for histones at basic pH later acid abstraction of DNA. It is widely employed in electrophoresis. It is used in food industries to colour fish, deserts, sauces, jellies and vegetables. As far as we know no effort was made to remove it from the sonophotocatalytic approach.

Only ZnO was employed on degradation of Acid red 14 dye and degradation rate was 70.4% in 3.5 h by only photocatalysis²¹. Rhodamine B degradation by only ZnO sonocatalytically was found to be 39.1%²². While we achieve 100% degradation and 76% COD removal in 1.66 h.

Acknowledgement

The authors are thankful to DST FIST schemes of the Department of Physics, M. L. Sukhadia University, Udaipur for providing XRD characterization. Moreover, we are grateful to UGC-DAE Consortium, Indore for sanctioning TEM facility and SAIF Chandigarh for providing FESEM, EDX, UV-DRS facilities. Thanks to HOD, Department of Chemistry, M. L. Sukhadia University, Udaipur for serving research laboratory facilities. We are also grateful to Professor Sudhish Kumar for his guidance in evaluation of band gap during the research. This research does not obtain any scholarship from finance agencies from any commercial, community, or non-profit sectors.

References

1. S. Madhav, A. Ahamad, P. Singh and P. K. Mishra, *Environ. Qual. Manag.*, 2018, **27**, 31.
2. G. Sharma, S. Bhogal, M. Naushad, Inamuddin, A. Kumar and F. J. Stadler, *J. Photochem. Photobiol. A: Chem.*, 2017, **347**, 235.
3. Y. Andolsi and F. Chaabouni, *J. Alloys Comp.*, 2019, **818**, 152739.
4. A. A. Mohanan and N. Ramakrishnan, *Microsyst. Technol.*, 2020, **26**, 2075.
5. R. Duarah and N. Karak, *Chem. Eng. J.*, 2019, **370**, 716.
6. K. Micheal, A. Ayeshamariam, S. Devanesan, K. Bhuvanewari, T. Pazhanivel, M. S. AlSalhi and M. J. Aljaafreh, *J. King Saud Univ. Sci.*, 2019, **32**, 1081.
7. M. M. Rahman, *Sens. Actuators B: Chem.*, 2019, **305**, 127541.
8. L. Zhang, L. Du, X. Yu, S. Tan, X. Cai, P. Yang, Y. Gu and W. Mai, *ACS Appl. Mater.*, 2014, **6**, 3623.
9. P. Mitra, D. Dutta, S. Das, T. Basu, A. Pramanik and A. Patra, *ACS Omega*, 2018, **3**, 7962.
10. O. Sacco, D. Sannino and V. Vaiano, *Appl. Sci.*, 2019, **9**, 472.
11. Y. Yu, J. Geng, H. Li, R. Bao, H. Chen, W. Wang, J. Xia and W.-Y. Wong, *Sol. Energy Mater. Sol. Cells*, 2017, **168**, 91.
12. S. Kundu and A. Patra, *Chem. Rev.*, 2016, **117**, 712.
13. S. Moseh and M. R. Rahimi, *Ultrason. Sonochem.*, 2017, **35**, 449.
14. S. Natarajan, H. C. Bajaj and R. J. Tayade, *J. Environ. Sci.*, 2018, **65**, 201.
15. L. Carmine, A. Ancona, K. Di Cesare, B. Dumontel, N. Garino, G. Canavese, S. Hernández and V. Cauda, *Appl. Catal. B: Environ.*, 2018, **243**, 629.
16. M. Dastkhon, M. Ghaedi, A. Asfaram, A. Goudarzi, S. M. Mohammadi and S. Wang, *Ultrason. Sonochem.*, 2017, **37**, 94.
17. H. Ferkous, S. Merouani, O. Hamdaoui and C. Pétrier, *Ultrason. Sonochem.*, 2017, **34**, 580.
18. G. Eshaq, S. Wang, H. Sun and M. Sillanpää, *Sep. Purif. Technol.*, 2019, **231**, 115915.
19. M. Sun, Y. Yao, W. Ding and S. Anandan, *J. Alloys Comp.*, 2019, **820**, 153172.
20. S. Kumawat, K. Meghwal, S. Kumar, R. Ameta and C. Ameta, *Water Sci. Technol.*, 2019, **80**, 1466.
21. N. Daneshvar, D. Salari and A. Khataee, *J. Photochem. Photobiol. A: Chem.*, 2004, **162**, 317.
22. J. Wang, Z. Jiang, Z. Zhang, Y. Xie, X. Wang, Z. Xing, R. Xiu and X. Zhang, *Ultrason. Sonochem.*, 2008, **15**, 768.